Available online at www.sciencedirect.com
ScienceDirect
European Polymer Journal 42 (2006) 2205–2210
EUROPEAN POLYMER JOURNAL
www.elsevier.com/locate/europolj

Macromolecular Nanotechnology

Single light emitters in electrospun polymer nanofibers: Effect of local confinement on radiative decay

Nikodem Tomczak [a], Shuying Gu [a], Mingyong Han [c,d], Niek F. van Hulst [b,*,1], G. Julius Vancso [a,*]

[a] *Materials Science and Technology of Polymers, Faculty of Science and Technology and MESA+ Institute for Nanotechnology, University of Twente, P.O. Box 217, 7500 AE Enschede, The Netherlands*
[b] *Applied Optics Group, Faculty of Science and Technology and MESA+ Institute for Nanotechnology, University of Twente, P.O. Box 217, 7500 AE Enschede, The Netherlands*
[c] *Division of Bioengineering, National University of Singapore, Singapore 117576, Singapore*
[d] *Institute of Materials Research and Engineering, 3 Research Link, Singapore 117602, Singapore*

Received 18 May 2006; accepted 18 June 2006
Available online 23 August 2006

Abstract

The fabrication of light emitting polymer nanofibers by electrospinning of polymer solutions containing either fluorescent organic dye molecules or luminescent semiconductor nanoparticles (quantum dots) is presented. The fluorescence spectra and lifetime of the embedded emitters, down to the level of single molecules were investigated. While the average fluorescence lifetime of single molecules embedded in poly(methyl methacrylate) fibers appears independent of the fiber diameter, the single molecule approach reveals a significant broadening of the fluorescence lifetime distribution for fibers with diameters below the wavelength of light.

Keywords: Electrospinning; Quantum dots; Single molecule; Fluorescence lifetime

1. Introduction

Polymer nanofibers are promising candidates for next generation photonic devices [1]. For example, fibrous dielectric nanostructures can be used as single mode light waveguides, sensors [2] or building blocks of photonic bandgap materials [3]. For a number of applications, it is important to have access to technologies, which allow one to introduce light emitters into the fibers, with simultaneous control over the location and amount of the emitters, down to the single molecule level. Despite growing importance, the optical properties of light emitters embedded in polymer nanofibers have so far not been explored in depth, due to technological challenges in obtaining fibers with diameters in the

* Corresponding authors. Fax: +34 935534000 (Niek F. van Hulst); fax: +31 534893823 (G. Julius Vancso).
E-mail addresses: niek.vanhulst@icfo.es (N.F. van Hulst), g.j.vancso@utwente.nl (G. Julius Vancso).
[1] Present address: ICFO – Institut de Ciències Fotòniques, Parc Mediterrani de la Tecnologia, Av. del Canal Olímpic s/n 08860 Castelldefels, Barcelona, Spain.

0014-3057/$ - see front matter © 2006 Elsevier Ltd. All rights reserved.
doi:10.1016/j.eurpolymj.2006.06.017

range of the wavelength of light. Electrospinning of polymer solutions and melts is an attractive technique to fabricate polymer fibers with diameters ranging approximately from ten nanometers to several micrometers [4–8]. A major advantage of electrospinning is the possibility to produce hybrid, functional photonic materials by incorporating e.g., light emitters into the fibers [9,10]. The polymer, the light emitter and the characteristic size of the structures can be varied independently, therefore allowing for a wide range of applications. Both organic dye molecules and inorganic materials can be embedded into the fibers. Particularly, semiconductor nanoparticles – quantum dots (QD) – are an interesting class of light sources, because of their size tunable optical properties, narrow emission lines and low photobleaching rates [11]. These properties make QDs also an attractive choice as light sources for optoelectronics [12], lasers [13], or biotechnological applications [14–16].

Photonic structures with wavelength-scale dimensions offer interesting opportunities to engineer the optical properties of embedded emitters, which depend strongly on the surrounding of the light emitters [17,18]. Particularly, for dimensions approaching the wavelength of light, the associated strong modification of the local photonic density of states alters the photophysical properties of the emitters. Similarly, fluorophores deposited on surfaces [19], placed close to a metallic mirror [20,21] or embedded in dielectric particles [22] were shown to display different radiative decay rate, quantum yield and photobleaching rate. Besides the size of the structures also the position of the light emitter within the structures and the orientation of the emission dipole moment with respect to the interfaces (electromagnetic boundaries) play a substantial role [23,24].

In this letter we present a study at the single light emitter level [25] as a first step towards investigations of the influence of the cylindrical dielectric geometry on the optical properties of the embedded chromophores. We show here how electrospinning is used to prepare hybrid, luminescent nanofibers. Fluorescent molecules and luminescent semiconductor nanoparticles (quantum dots) are embedded into fibers with diameters ranging from 50 nm to several micrometers. We show the influence of the fiber diameter on the single molecule fluorescence lifetime (τ_f) distributions of the embedded chromophores. For diameters of fibers below 500 nm a significant broadening of τ_f distributions is observed.

2. Experimental section

The electrospinning device used in this study consisted of a capillary (tip diameter 2 mm), which included a wire electrode, a grounded counter electrode placed 12 cm from the capillary and a high voltage source. The potential between the electrodes was adjusted with a high-voltage power supply (Bertan Series 230). More details about the electrospinning device used in this study can be found elsewhere [26,27]. Luminescent polymer fibers were prepared by electrospinning poly(ethylene oxide) (PEO, $M_w = 2000$ kg/mol, Aldrich) and PMMA ($M_w = 120$ kg/mol, Aldrich) solutions containing 1,1′,3,3,3′,3′-hexamethylindodicarbocyanine ($DiIC_1(5)$) molecules (Molecular Probes, D-307) or CdSe/ZnS core-shell semiconductor nanoparticles (preparation method of the nanoparticles can be found in references [28,29]). To be able to perform subsequent optical investigations, a transparent substrate (circularly shaped glass cover slides, Ø = 20 mm, Fisher Scientific) was placed on the counter electrode in the path of the ejected fibers. Prior to electrospinning, the slides were cleaned using Piranha solution (mixture of 1:4 of 30% H_2O_2 and concentrated H_2SO_4), rinsed with Milli-Q water and ethanol, and finally dried in a stream of nitrogen gas. For efficient collection, the cover slides were placed off-axis with respect to the capillary. The amount of the fibers deposited on the cover slides was controlled by the spinning time.

The resulting luminescent fibers were examined by scanning confocal microscopy [30]. For excitation of the embedded chromophores picosecond-pulsed dye lasers (PicoQuant, 800-B, 80 MHz repetition rate) emitting at 635 nm and 476 nm or a CW Ar^+/Kr^+ ion laser (Spectra Physics, Beamlok 2060) emitting at a wavelength of 514 nm was used. Before entering the microscope, the excitation light was made circularly polarized by a $1/4\lambda$ plate and focused onto the sample to a diffraction-limited spot using a high NA oil objective (Olympus, NA=1.4, $100x$). To separate the fluorescence emission from the excitation, suitable dichroic mirrors, emission, and excitation filters, were used. Fluorescence photons were collected by the same objective and split into two paths. The first path went to two avalanche photodetectors (SPCM-AQ-14, EG&G Electro Optics) placed after a polarization beam splitter (splitting into two orthogonal components). The fluorescence photons in the second path were directed to a prism and dispersed on a cooled CCD

camera to obtain fluorescence emission spectrum. Fluorescence spectra were obtained by integrating the arriving photons over a period of 1 s. A custom-built piezo-scan table with an active x–y feedback loop mounted on a commercial optical microscope (Zeiss Axiovert inverted microscope) was used. The sample was scanned through the focus of the excitation spot at a pixel frequency of 1 kHz, producing two-dimensional (256×256 pixels) fluorescence intensity images (including two independent polarization channels, when required). Custom LabView software was used to control the scanning process and for data acquisition. For time-resolved experiments the detected fluorescence signal was fed into a time-correlated single photon-counting card (TCSPC, SPC 500). All experiments were performed in air under ambient conditions.

3. Results and discussion

In electrospinning, when a potential is applied between two electrodes, the liquid droplet suspended at the end of the capillary thins and forms a so-called "Taylor cone" [31]. By increasing the potential further, the surface tension of the liquid is being overcome and the liquid is ejected towards the counter electrode. The diameter and morphology of the resulting fibers depend on a number of parameters including solution viscosity, surface tension, applied voltage and the distance between the electrodes. In Fig. 1 scanning electron microscopy (SEM) images of electrospun PMMA fibers are presented. Spinning the polymer solutions at 20 kV (Fig. 1(a)) resulted in uniform fibers with a broad distribution of the fiber diameter values (as measured with an Atomic Force Microscope; not shown here). Beaded PMMA fibers were also observed, however, when the applied voltage between the electrodes was decreased to 16 kV, and lower (Fig. 1(c)). Such bead-on-a-string morphology [32] is also interesting for photonic applications, and a more detailed study of the photonic properties of beaded fibers is presented elsewhere [33].

The concentration of the light emitters in the fibers was controlled by adding to the polymer solution various concentrations of chromophores. Addition of low molar mass organic chromophores or semiconductor nanoparticles to the initial spinning solution had no visible influence on the fiber morphology and diameter (Fig. 1(b)).

Fig. 2(a) shows a $10 \times 10\ \mu m^2$ fluorescence intensity scan of luminescent $DiIC_1(5)$/PEO fibers. The

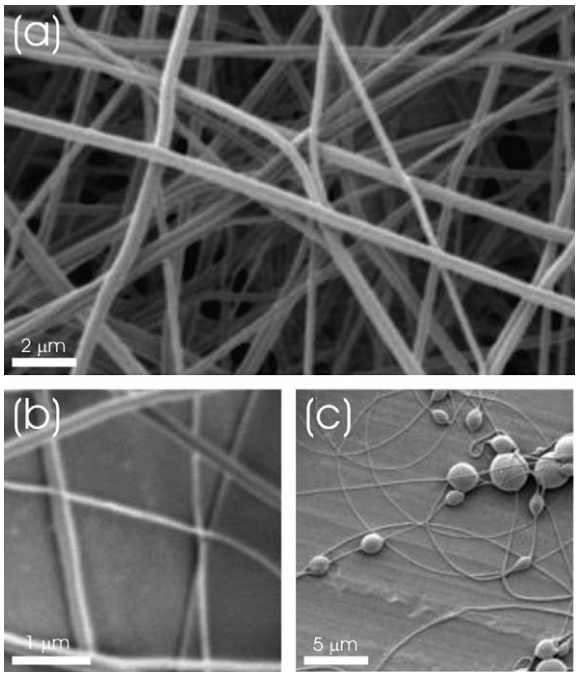

Fig. 1. SEM images of electrospun PMMA fibers prepared from (a) 20 wt% PMMA solution in DMF, spun at a potential of 20 kV, (b) 20 wt% PMMA solution with $DiIC_1(5)$ dyes in a 10^{-3} M concentration in the initial spinning solution and (c) 18 wt% PMMA solution in DMF spun at a potential of 16 kV.

fluorescent molecules are uniformly distributed within and along the fibers. Fluorescence spectra taken from individual fibers confirmed that the optical signal comes from $DiIC_1(5)$ molecules (Fig. 2(c)). A small red shift of the emission of about 10 nm when compared to a bulk solution is observed and attributed to the different dielectric properties of the surroundings (solvent versus polymer). By decreasing the concentration of the chromophores in the initial spinning solution (down to 10^{-11} M), observations of $DiIC_1(5)$ at the single molecule level were possible (Fig. 2(e)). We have also embedded CdSe/ZnS core-shell semiconductor nanoparticles (Fig. 2(b)) into electrospun fibers made of PMMA and PEO. Fig. 2(b) shows a PEO/QD composite fiber with a high concentration (10^{-5} M) of the quantum dots. The QDs are also uniformly distributed over the length and width of the fiber. Fluctuations in the QD emission intensity visible on the scan are due to frequent blinking of the quantum dots [34]. By decreasing the QD concentration in the initial spinning solution (down to 10^{-8} M) we decreased the amount of the nanoparticles in the fibers to the level such that single nanoparticles were separated in the fibers (Fig. 2(f)).

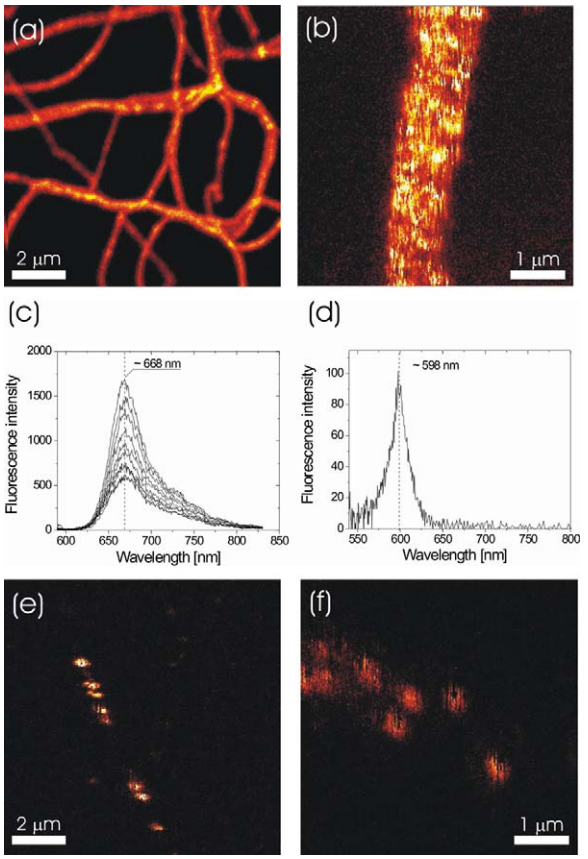

Fig. 2. Scanning confocal fluorescence images of (a) $DiIC_1(5)$ and (b) CdSe/ZnS quantum dots embedded in electrospun PEO fibers. The chromophores are distributed uniformly within and along the fibers, (c) Fluorescence emission spectra taken from individual fibers with embedded $DiIC_1(5)$ molecules, (d) emission spectrum of an individual QD embedded in a PEO fiber, and (e, f) single $DiIC_1(5)$ molecules and QDs along PMMA fibers. Characteristic blinking behavior is clearly visible and indicates that the fluorescence is coming from single light emitters.

The full-width at half-maximum of the intensity cross-section through an isolated fluorescence spot was equal to ~300 nm, slightly larger than expected for a diffraction limited spot (~220 nm) when imaged with a 1.4 NA objective. The reason for the broadening is most probably related to the size of the focus of the excitation light during imaging. Fig. 2(d) shows the emission spectrum of a single QD. The emission peaks around 600 nm, at the same wavelength as obtained from a bulk solution of QD in chloroform. However, comparing with the solution spectrum the full width at half maximum of the emission peak for a single QD is equal to 22 nm and is 78% of that found in a chloroform solution. The narrower emission spectrum of single QDs within the fibers is probably due to the size polydispersity of the QDs causing the solution spectrum to look broader [34].

Having developed a method to obtain polymer fibers with embedded chromophores we turned our attention towards more detailed investigations of the optical properties of the structures obtained, specifically the fluorescence lifetime and the effect of electromagnetic boundaries. Here we report on the investigation of the fluorescence lifetime of single molecules as a function of the polymer fiber diameter. By parking the molecules at the focus of the excitation, and using a time-correlated single-photon counting module, the fluorescence lifetime (τ_f) of single $DiIC_1(5)$ molecules was obtained. A histogram of fluorescence lifetime values was subsequently built from at least 50 single molecules for each fiber diameter investigated.

Fig. 3 shows single molecule fluorescence lifetime histograms of $DiIC_1(5)$ molecules as a function of the polymer fiber diameter. For fiber diameters below ~400 nm the size was hard to determine due to diffraction. Therefore, we have grouped all fluorescent lifetime results for such fibers into one

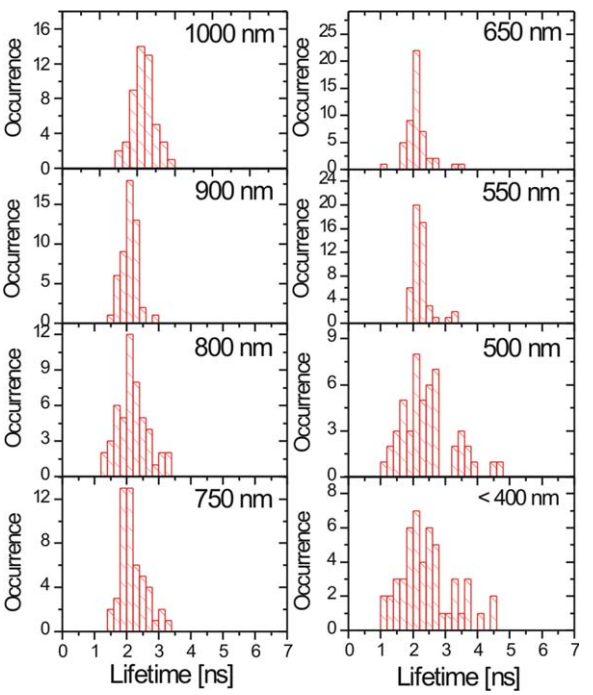

Fig. 3. Single molecule fluorescence lifetime histograms of $DiIC_1(5)$ embedded in PMMA fibers as a function of the polymer fiber diameter. Below 500 nm the distributions become significantly broader.

histogram in Fig. 3 (<400 nm). For fiber diameters above 500 nm the mean fluorescence lifetime of the $DiIC_1(5)$ molecules is almost independent of the fiber diameter and its value is centered around 2.0–2.2 ns. The widths of the distributions are relatively narrow, but still significant compared to the accuracy of the experimental lifetime value (~0.3 ns). Although the mean value of τ_f for fibers with diameter smaller than 500 nm is similar to the rest of the fiber diameters, a significant broadening of the τ_f distributions is observed for lower fiber diameters. The broadening is slightly asymmetric towards higher lifetime values and occasionally fluorescence lifetime values as high as 4.5 ns were observed. To appreciate the broadening, we show in Fig. 4 the mean values of the τ_f distributions. The horizontal bars represent the widths of the fluorescence lifetime distributions. Clearly, a drastic broadening of the distributions is already visible for fibers with a diameter of 500 nm. Surprisingly, the change in the width values is rather abrupt and occurs within a variation of 50 nm in the fiber diameter.

It is known that the presence of dielectric interfaces influences the radiative transition frequencies and decay rates [23,35]. For thin films, longer fluorescence lifetimes were found for single molecules closer to the dielectric/air interface and with transition dipole moments oriented perpendicular to the interfaces [24,35]. In fibers a substantially higher amount of molecules (within the distributions) can be present with their dipole moments perpendicular to the interfaces, as compared to thin films, due to the quasi one-dimensional morphology of the fibers. In addition, for a cylindrical geometry, the molecules are on average closer to the interfaces for thinner fibers. Molecules with their transition dipole moments oriented perpendicularly to the interfaces and located just at the polymer/air boundary would also show lower lifetime values. Therefore, one can relate the broadening towards both higher and lower fluorescence lifetime values with decreasing fiber diameter to electromagnetic boundary condition (EBC) effects. However, it is difficult to estimate the exact location of the dyes with respect to the fiber walls. Additional experiments with in-situ measurements of the fiber diameter by AFM should shed more light on the origin of the results obtained.

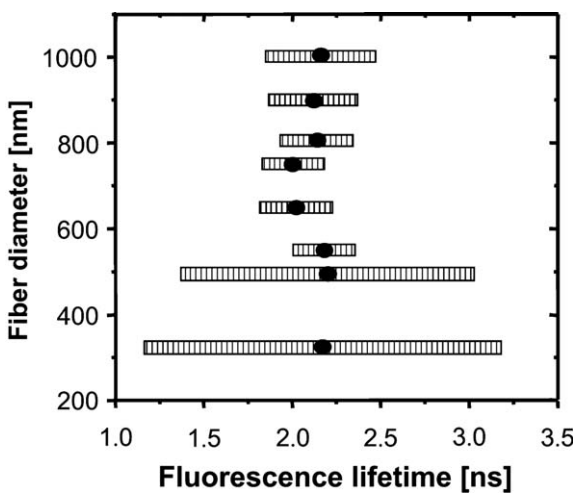

Fig. 4. Mean values of τ_f distributions as a function of fiber diameter. The horizontal bars represent the widths of the τ_f distributions. Significant broadening of the distributions for fiber diameters of 500 nm and below is clearly visible.

4. Conclusions

We have prepared luminescent micro- and nanofibers by electrospinning. Fluorescent molecules and luminescent CdSe/ZnS core-shell semiconductor nanoparticles were embedded into polymer fibers with diameters ranging from 50 nm to several microns. The fluorescence lifetime of single $DiIC_1(5)$ molecules embedded in PMMA fibers was found to be independent of the fiber diameter. However, significant broadening of the single-molecule fluorescence lifetime distributions was observed for fibers with diameter values below 500 nm. A possible explanation for the broadening observed was the modification of the radiative decay rates through the effect of the electromagnetic boundary conditions.

Acknowledgements

We thank Lanti Yang for her experimental work with electrospinning. The Council for Chemical Sciences of the Netherlands Organization for Scientific Research (NWO-CW) is acknowledged for financial support of this research.

References

[1] Shen Y, Prasad PN. Appl Phys B 2002;74:641.
[2] Wang XY, Drew C, Lee SH, Senecal KJ, Kumar J, Samuelson LA. Nano Lett 2002;2:1273.
[3] Dersch R, Steinhart M, Boudriot U, Greiner A, Wendorff JH. Polym Adv Technol 2005;16:276.
[4] Formhals A. 1938. US Patent 2,116,942.
[5] Doshi J, Reneker DH. J Electrostat 1995;35:151.

[6] Reneker DH, Chun I. Nanotechnology 1996;7:216.
[7] Jaeger R, Schönherr H, Vancso GJ. Macromolecules 1996;29:7634.
[8] Bognitzki M, Czado W, Frese T, Schaper A, Hellwig M, Steinhart M, et al. Adv Mater 2001;13:70.
[9] Schlecht S, Tan S, Yosef M, Dersch R, Wendorff JH, Jia Z, et al. Chem Mater 2005;17:809.
[10] Wang XY, Lee SH, Ku BC, Samuelson LA, Kumar J. Macromol Sci 2002;A39:1241.
[11] Alivisatos AP. Science 1996;271:933.
[12] Colvin VL, Schlamp MC, Alivisatos AP. Nature 1994;370:354.
[13] Klimov VI, Mikhailovsky AA, Xu S, Malko A, Hollingsworth JA, Leatherdale CA, et al. Science 2000;290:314.
[14] Weiss S. Science 1999;283:1676.
[15] Chan WCW, Maxwell DJ, Gao XH, Bailey RE, Han MY, Nie SM. Curr Opin Biotech 2002;13:40.
[16] Han MY, Gao XH, Su JZ, Nie SM. Nat Biotech 2001;19:631.
[17] Purcell EM. Am Phys Soc 1946;69:681.
[18] Drexhage KH. J Lumin 1970;12:693.
[19] Macklin JJ, Trautman JK, Harris TD, Brus LE. Science 1996;272:255.
[20] Danz N, Heber J, Brauer A, Kowarschik R. Phys Rev A 2002;66:063809.
[21] Vasilev K, Knoll W, Kreiter M. J Chem Phys 2004;120:3439.
[22] Schniepp H, Sandoghdar V. Phys Rev Lett 2002;89:257403.
[23] Lukosz W, Kunz RE. J Opt Soc Am 1977;67:1607.
[24] Kreiter M, Prummer M, Hecht B, Wild UP. J Chem Phys 2002;117:9430.
[25] For a recent review of single-molecule optical detection (SMD) and spectroscopy methods see Kulzer F, Orrit M. Annu Rev Phys Chem 2004;55:585.
[26] Jaeger R, Bergshoef MM, Batlle CMI, Schönherr H, Vancso GJ. Macromol Symp 1998;127:141.
[27] Bergshoef MM, Vancso GJ. Adv Mater 1999;11:1362.
[28] Dabbousi BO, Rodriguez-Viejo J, Mikulec FV, Heine JR, Mattoussi H, Ober R, et al. J Phys Chem B 1997;101:9463.
[29] Qu L, Peng X. J Am Chem Soc 2002;124:2049.
[30] García-Parajó MF, Veerman JA, Bowhuis R, Vallée RAL, van Hulst NF. Chem Phys Chem 2001;2:347.
[31] Jayaraman K, Kotaki M, Zhang YZ, Mo XM, Ramakrishna S. J Nanosci Nanotech 2004;4:52.
[32] Fong H, Chun I, Reneker DH. Polymer 1999;40:4585.
[33] Tomczak N, van Hulst NF, Vancso GJ. Macromolecules 2005;38:7863.
[34] Empedocles SA, Neuhauser R, Shimizu K, Bawendi MG. Adv Mat 1999;11:1243.
[35] Vallée RAL, Tomczak N, Gersen H, van Dijk EMHP, García-Parajó MF, Vancso GJ, et al. Chem Phys Lett 2001;348:161.